Deep-Learning-Based Radio Map Reconstruction for V2X Communications

Sandra Roger, *Senior Member, IEEE*, Mattia Brambilla, *Member, IEEE*, Bernardo Camajori Tedeschini, *Graduate Student Member, IEEE*, Carmen Botella-Mascarell, *Senior Member, IEEE*, Maximo Cobos, *Senior Member, IEEE*, and Monica Nicoli, *Senior Member, IEEE*

***Abstract*—Radio environment map (REM) reconstruction based on large-scale channel measurements is a promising technology for future mobility services involving vehicle-to-everything (V2X) communications. REMs provide contextual information which can be exploited to reduce V2X communication latency and control signaling, for instance, through a fast access to channel state information. However, the accuracy of radio mapping techniques is limited by the availability of measurements, which require for collection significant signaling overhead. Moreover, mobility scenarios impose strict latency constraints that render fast channel acquisition a challenging problem. This paper presents a low-complexity deep-learning-based approach based on long-short term memory (LSTM) cells for REM reconstruction on roads, addressed as a data-filling problem. To improve model generalization, the network is trained on a virtually infinite dataset generated according to a 3GPP-compliant freeway scenario, considering different correlation properties and missing point configurations. The results show that the proposed approach provides a performance closer to the theoretical lower bound than the classical Ordinary Kriging spatial interpolation method, without increasing the complexity order. Experiments performed in realistic scenarios using a 3D city model confirm the generalization capability of the proposed solution.**

***Index Terms*—Deep learning, radio environment maps (REMs), RNN, vehicle-to-everything (V2X), vehicular communications.**

I. Introduction

SPATIAL channel interpolation techniques have recently gained interest in beyond 5G (B5G) or 6G vehicle-to-everything (V2X) applications due to their ability to reconstruct the radio environment map (REM) of a given base station (BS) from a subset of available measurements [1]. Although REMs were originally proposed as a solution for cognitive radio systems [2], they are currently considered as a key enabler for radio environmental awareness [3]. Vehicular services often involve groups of vehicles communicating in close proximity, such as the vehicles travelling in a platoon or those performing cooperative collision avoidance [4]. In such applications, the contextual information provided by REMs can offer several advantages, for instance, reducing the control signaling necessary for channel estimation, as shown in a platooning use case in [5].

Many techniques for spatial interpolation can be found in the literature, such as nearest neighbor [6], inverse distance weighting [6], [7], natural neighbor [8], thin plate splines [8], Gaussian process regression [9], [10], [11] and Kriging [1], [6], [7], [8], [12], [13], [14], [15]. Specifically, Kriging is a method that was originally used in geostatistics, but it has been applied since then in many fields, and it is currently widely used for REM reconstruction. Prior art has proved the superior performance of Kriging under different evaluations metrics versus various methods such as nearest neighbor and inverse distance weighting techniques (see [6], [15]), natural neighbor (see [1]) and, more recently, over 1D interpolation techniques based on piecewise cubic Hermite interpolating polynomials [5].

A number of solutions based on channel parameter learning have been recently proposed for REM reconstruction [16], [17], [18], [19], [20], [21]. In [16], neural networks are used to estimate the path-loss, while Kriging estimates the shadowing value. Reference [17] discusses the complexity related to deep learning (DL) methods and models REM reconstruction as a shadowing adjustment problem by considering the REM as an image. An advanced solution for multi-domain reconstruction including space, time or frequency can be found in [18]. Authors in [21] proposed a DL method for estimating the propagation path-loss from a transmitter. The method learns from a physical simulation dataset, and generates path-loss estimations that are very close to the simulations. Finally, the survey works in [19], [20] provide a wide overview of REM reconstruction methods, with examples covering both classical and more advanced DL-based solutions.

In this work, we target the estimation of the large-scale channel losses between a target BS and a set of connected vehicles passing by its coverage area. Prior work has solved this

Manuscript received 15 May 2023; revised 6 September 2023; accepted 19 October 2023. Date of publication 23 October 2023; date of current version 14 March 2024. This work was supported in part by MCIN/AEI/10.13039/501100011033 under Grants PID2020-113785RB-100 and RYC-2017-22101, in part by MCIN/AEI/10.13039/501100011033 and European Union NextGenerationEU/PRTR under Grant TED2021-131003B-C21, in part by the Generalitat Valenciana of Spain under Grant CIAICO/2022/179, and in part by the Ministerio de Universidades of Spain under Grant CAS21/00096. The review of this article was coordinated by Dr. Zilong Liu. *(Corresponding author: Sandra Roger.)*

Sandra Roger, Carmen Botella-Mascarell, and Maximo Cobos are with the Computer Science Department, Universitat de València, 46100 Burjassot, Spain (e-mail: sandra.roger@uv.es; carmen.botella@uv.es; maximo.cobos@uv.es).

Mattia Brambilla and Bernardo Camajori Tedeschini are with the Department of Electronics, Information and Bioengineering, Politecnico di Milano, 20133 Milan, Italy (e-mail: mattia.brambilla@polimi.it; bernardo.camajori@polimi.it).

Monica Nicoli is with the Department of Management, Economics and Industrial Engineering, Politecnico di Milano, 20156 Milan, Italy (e-mail: monica.nicoli@polimi.it).

Digital Object Identifier 10.1109/TVT.2023.3326935

problem using Kriging interpolation [5]. However, the Kriging method heavily relies on semivariogram modeling, which strongly depends on the particular geometry of the problem under consideration, as pointed out in [5]. Moreover, the number of available measurements for interpolations is low and the correlation between samples plays then a fundamental role. Note that, as derived in [1], a solution based on Kriging needs at least three available samples to start the reconstruction process, besides a prior knowledge of the correlation level. Given the considered vehicular scenario, which imposes strict latency constraints, our aim is the design of a low complexity DL-based estimation method with a reduced number of parameters. Moreover, the model should by easily adapted and retrained to meet the requirements of a particular deployment, while featuring good generalization capabilities as well. To this end, we pursue the reconstruction of a set of unknown large-scale channel values through a recurrent neural network (RNN) architecture. RNNs have been extensively studied in the context of speech and language processing [22], and Long-Short Term Memory (LSTM) architectures, which are built and optimized on the basis of RNNs, have shown to be powerful methods to deal with time-series processing tasks aimed at the discovery of temporal relationships. Our proposal exploits the particularities of a typical freeway geometry and considers data generated from a path-loss model. We also impose this estimator to be completely blind and adaptive, i.e., it should predict the unknown field values without knowledge on the specific correlation level between the field values. The hypothesis is that the RNN architecture, by exploiting the existing spatial relationships within a number of incomplete field observations, will learn the underlying large-scale channel model to reconstruct the missing information.

Specifically, the key contributions of this paper are:

- A low-complexity LSTM-based method for REM reconstruction, together with a simple yet effective training procedure that allows for a blind estimation of the received signal power under deployments with different correlation properties.
- A benchmarking with a theoretical lower bound on the estimation performance. In contrast to many DL-based proposals where either the nature or the dimensionality of the problem to solve makes unfeasible to obtain a theoretical lower bound, the proposed architecture is designed and evaluated with awareness of the lowest achievable error.
- A comparison with the well-known Kriging algorithm for spatial interpolation, establishing a reference performance representative of classical state-of-the-art approaches.
- An analysis of the performance over realistic 3D urban and freeway scenarios, assessing the method generalization capabilities.

The remainder of the paper is structured as follows. Section II introduces the system model considered in this work. Section III discusses the proposed LSTM-based REM reconstruction scheme. A lower bound analysis is presented in Section IV. Finally, numerical results are shown in Section V, and some conclusions and future research directions are drawn in Section VI.

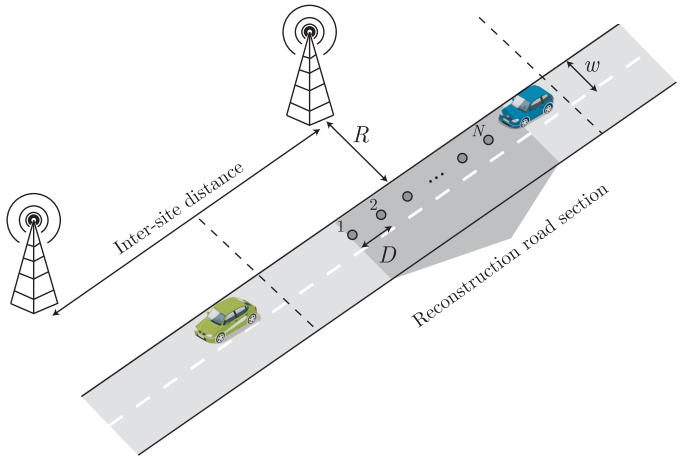

Fig. 1. Scenario under consideration.

II. System Model

A. Scenario

We focus on a Third Generation Partnership Project (3GPP)-compliant vehicular scenario to simulate V2X communications in a straight segment of a freeway [23]. BSs are deployed along the freeway, at a distance R from the road border and with an inter-site distance equal to 1732 m [23] (see Fig. 1). Without loss of generality, the BS of interest is located at the origin of the cartesian spatial reference system. Throughout the paper, we will refer to vehicle positions or antenna positions indistinctly. As an usual assumption, the vehicle antennas are located in the middle of the roof, assuming, for simplicity, that their position matches the middle point of the vehicle in both directions.

B. Radio Environment Map Reconstruction Problem

Let us consider a uniform spatial sampling of the received signal power along a target area of the reference road scenario depicted in Fig. 1. We consider the average power, i.e., the power that is obtained by averaging over time the fast fading and that includes only shadowing and static multipath components. The received power value at a vehicle located at position $\mathbf{x}_i$ is denoted by $V(\mathbf{x}_i)$, where $\mathbf{x}_i$ pertains to the set $\mathcal{S}$ containing all the considered road locations, i.e., $\mathcal{S} = \{\mathbf{x}_i,\, i = 1, \ldots, N\}$. In the problem at hand, only P out of the N power values are available, so the set $\mathcal{S}$ can be divided into the union of two sets containing the positions with known and unknown field values, i.e., $\mathcal{S} = \mathcal{K} \cup \mathcal{U}$, with cardinalities $|\mathcal{K}| = P$ and $|\mathcal{U}| = N - P$, respectively.

Available field values, i.e., received power due to large-scale channel effects in this work, can be acquired either through a conventional channel acquisition stage, or through queries to a previously stored database containing the REM of the area. The aim of the method here proposed is to achieve REM reconstruction for the unknown positions in $\mathcal{U}$ given the power readings at $\mathcal{K}$. We assume the positions are perfectly known, i.e., we disregard any Global Positioning System error.

The position-dependent field value $V(\mathbf{x}_i)$, which includes large-scale channel losses in logarithmic units (dBm), results

from the sum of two contributions:

$$V(\mathbf{x}_i) = P_r(\mathbf{x}_i) + S_\sigma(\mathbf{x}_i), \tag{1}$$

where $P_r(\mathbf{x}_i)$ is the average received power and $S_\sigma(\mathbf{x}_i)$ is the shadow fading following a zero mean normal distribution with σ^2 variance, i.e., log-normal in the linear scale [24]. In the model we assume that the shadow fading is spatially correlated between positions $\mathbf{x}_i$ and $\mathbf{x}_j$, with correlation equal to:

$$R_{ij} = \mathrm{E}\left[S_\sigma(\mathbf{x}_i) S_\sigma(\mathbf{x}_j)\right] = \sigma^2 \rho_{ij}, \tag{2}$$

being ρ_{ij} the correlation coefficient modelled as [25]

$$\rho_{ij} = \exp\left(-\frac{\|\boldsymbol{x}_i - \boldsymbol{x}_j\|_2}{L_c}\right). \tag{3}$$

Note that L_c is the decorrelation distance in meters, defined as the distance satisfying $\rho_{ij} = 1/e \approx 0.37$ [23].

The average received power at location $\mathbf{x}_i$ from a single-antenna BS is considered to follow the simplified path-loss model [24]:

$$P_r(\mathbf{x}_i) = P_t + K_{\mathrm{dB}} + 10\,\alpha \log_{10}\left(\frac{d_0}{d_i}\right) \quad [\mathrm{dBm}], \tag{4}$$

where P_t is the transmitted power at the BS, K_{dB} is the constant path-gain factor in dB units at a reference distance d_0, α is the path-loss exponent, and d_i is the distance between the vehicle location $\mathbf{x}_i$ and the BS location. Note that, in this contribution, the small-scale fading effect is assumed to be averaged out by the receiver (see [26] for a discussion about this aspect). Hence, from now on, REM reconstruction will refer to the estimation of the large-scale fading channel effects (only path-loss and shadowing values).

III. LSTM-Based REM Reconstruction

A. LSTM-Based Estimation

Supervised DL-based REM reconstruction has been largely investigated [19], where neural networks are used to fill incomplete field observations by learning an appropriate mapping between the incomplete input and the actual complete map. Under the vehicular scenario considered in this work, the estimation task boils down to a time-series data-filling problem, where each time step actually corresponds to a spatial position. This problem can be efficiently handled by an RNN-based architecture by automatically learning the spatial relationships between the target power parameters.

We propose a neural network architecture that consists of an LSTM cell with M units acting as encoder, which takes as input a sequence of N field values, $\mathbf{v} \in \mathbb{R}_0^{+\,N\times 1}$, organized such that each of the elements of $\mathbf{v}$ corresponds to a given time step. The input vector $\mathbf{v}$ is constructed from the power loss readings at the known road locations, including a 0 value at those positions with an unavailable observation, i.e.:

$$v_i = \begin{cases} 0, & \text{if } \mathbf{x}_i \in \mathcal{U}, \\ P_t - V(\mathbf{x}_i), & \text{if } \mathbf{x}_i \in \mathcal{K}. \end{cases} \tag{5}$$

Note that we select the input to contain channel loss values instead of actual power measurements, to make the network independent from the BS transmitted power, which should be a known parameter within a realistic deployment framework. Also, as channel losses are always positive, unknown values can be safely encoded with zero values for not being feasible readings.

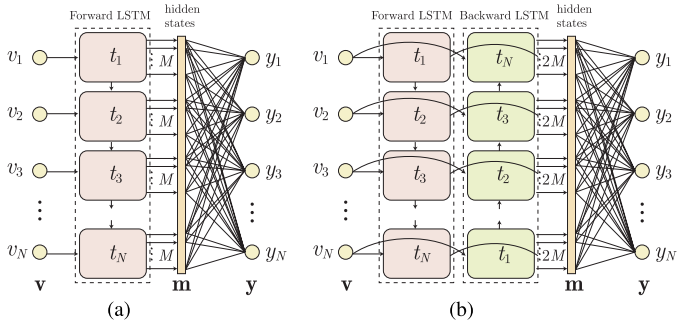

Fig. 2. Model architectures. (a) Unidirectional LSTM. (b) Bidirectional LSTM.

The output hidden states at each time step in the LSTM cell are flattened into a single vector representation $\mathbf{m} \in \mathbb{R}^{MN\times 1}$. The decoder is formed by a dense fully-connected layer with rectified linear unit (ReLU) activation that maps $\mathbf{m}$ into the filled output sequence $\mathbf{y} \in \mathbb{R}_0^{+\,N\times 1}$. A straightforward extension of the model is given by its bidirectional version, where the LSTM is applied twice by feeding a reversed version of the input (backward layer). In such case, the hidden states from both the forward and backward LSTMs are concatenated, so that $\mathbf{m} \in \mathbb{R}^{2MN\times 1}$. Both unidirectional and bidirectional models are graphically depicted in Fig. 2.

B. System Parameters

The parameters of a 3GPP-compliant freeway scenario are considered, where each lane has a width $w = 4$ m and the BSs are located $R = 35$ m away from the road border [23]. The carrier frequency is set to 5.9 GHz, as specified for vehicle-to-infrastructure communications in [23]. The original REM comprises the average received power values at N vehicle positions, obtained according to (1) and (4) particularized with the 3GPP parameters in [23]. More specifically, the constant path-gain factor is $K_{\mathrm{dB}} = -128.1$ dB for $d_0 = 1$ km, path-loss exponent takes the value $\alpha = 3.76$, and the shadowing contribution is drawn from a zero mean normal distribution with $\sigma = 8$ dB standard deviation. Since the focus is on the propagation parameters, the transmitted power is set to $P_t = 0$ dBm in the simulations for simplicity. Note that, in practice, the component leading to a higher degree of uncertainty in the received field value is given by the shadowing effect, more specifically, by the specific decorrelation distance of the considered scenario. This will motivate a training procedure where the network is tested on examples having different correlation parameters.

C. Training Procedure

The training of the network is performed by using an infinite synthetic dataset that generates power observations according to

the model described in Section II-B. To enhance the robustness of the method and improve generalization, a set of K increasing decorrelation distances is considered:

$$L_c^{(k)} = L_{\min} + k\frac{L_{\max} - L_{\min}}{K-1}, \quad k = 0, \ldots, K-1 \qquad (6)$$

where $L_{\min} = 25$ m and $L_{\max} = 50$ m, based on reported values for typical realistic scenarios [23]. In order to limit the complexity of the network, estimation is carried out along a road section of length $l_r = 2L_{\max}$. Considering an average passenger vehicle length of approximately 5 m, this separation between samples leads to input sequences of $N = 20$ estimation points. When dealing with non-uniformly spaced real measurements, samples are discretized in accordance with the chosen grid. This discretization process does not have a significant impact in the performance of the method, as the maximum discretization error (2.5 m) is small in comparison to $L_{\min}$. To account for distance effects, the sections are simulated by generating random offsets along the approximate BS coverage area on the road (inter-site distance).

For the purpose of creating input sequences with missing data at some locations, we consider different missing-data levels, with a number of available readings going from $P = 3$ (that is, only 3 known points, which is the minimum value to carry out interpolation with algorithms such as Ordinary Kriging) to $P = N - 1$ (only 1 missing point). The model is trained for 500 epochs by feeding mini-batches of 128 sequences with 2000 steps per epoch, using the Adam optimizer [27] with an initial learning rate of 0.01. The model is optimized by minimizing the mean squared error (MSE) between the complete target sequence and the neural network output.

D. Evaluation Procedure

Note that, for each P, there are $C_P = \binom{N}{P}$ possible combinations with P known values, leading to C_P possibilities for the associated sets $\mathcal{K}$ and $\mathcal{U}$. The MSE for a particular set of missing samples $\mathcal{U}$ is computed as:

$$\text{MSE} = \frac{1}{N-P}\sum_{\mathbf{x}_i \in \mathcal{U}} \left(\widehat{V}(\mathbf{x}_i) - V(\mathbf{x}_i)\right)^2 \quad [\text{dB}^2]. \qquad (7)$$

To make the performance evaluation independent from the specific configuration of missing values given a fixed P, we compute the average MSE over a large number of realizations comprising the C_P possible set combinations for $\mathcal{U}$, and denote it by MSE_P. Moreover, to summarize the overall performance over the considered range $P = 3, 4, \ldots, 19$, the global average MSE, indicated as $\overline{\text{MSE}}$, is also computed.

E. Model Selection

The specific combination of known samples could be either given by the practical situation, or set by a certain protocol. For instance, in some applications it may be useful to consider that the first P vehicles approaching the BS acquire their channel values, and the prediction is performed for the following consecutive $N - P$ positions. To train the models, we consider both options, either random combinations or combinations of consecutive samples. For evaluation, we test all the resulting models with the two types of combinations (random and consecutive).

TABLE I
UNIDIRECTIONAL LSTM (TRAINED ON RANDOM)

	$M = 32$	$M = 16$	$M = 8$	$M = 4$
Num. parameters	17172	7572	3540	1716
$\overline{\text{MSE}}$ [dB^2] (ev. random)	18.57	18.58	19.40	30.22
$\overline{\text{MSE}}$ [dB^2] (ev. consec.)	57.04	55.76	53.72	87.19

TABLE II
BIDIRECTIONAL LSTM (TRAINED ON RANDOM)

	$M = 32$	$M = 16$	$M = 8$	$M = 4$
Num. parameters	34324	15124	7060	3412
$\overline{\text{MSE}}$ [dB^2] (ev. random)	19.59	21.66	20.81	29.32
$\overline{\text{MSE}}$ [dB^2] (ev. consec.)	67.61	70.51	60.64	63.62

Both unidirectional and bidirectional LSTM architectures are investigated, varying the number of neurons in the main layer (M). The model is selected so as to minimize the target metric $\overline{\text{MSE}}$; in case of two models with a similar $\overline{\text{MSE}}$, the model with the lowest number of parameters and, thus, lowest complexity, is selected.

Table I shows the $\overline{\text{MSE}}$ values obtained with unidirectional LSTM networks with $M \in \{4, 8, 16, 32\}$ neurons, trained with random combinations of missing samples. The second row contains the results of the performance evaluation over random combinations (ev. random), whereas the third row contains the results after restricting to only consecutive combinations (ev. consec.). The resulting number of parameters of each model is included in the first row. It can be observed that the evaluation over random samples provides lower MSE values than the consecutive combinations case, which is consistent with the training assumption. The model with $M = 16$ has been recorded as the best option, since its performance with random combinations nearly matches the one of the $M = 32$ model, while outperforming the latter for the consecutive samples case.

Table II shows analogous evaluation results considering bidirectional LSTM models trained over random combinations of missing data. It can be observed that the bidirectional models cannot reduce the reconstruction error $\overline{\text{MSE}}$ compared to the unidirectional ones (see Table I), despite requiring to double the number of parameters of the network. Therefore, the initial unidirectional LSTM model with $M = 16$ remains the best option to reconstruct random combinations of missing data.

A similar analysis for the unidirectional and bidirectional models trained with only combinations of missing data in consecutive positions is shown in Table III. From the results in the second row, it can be observed that the models trained with consecutive combinations are not useful to reconstruct random combinations (reconstruction error $\overline{\text{MSE}}$ is above a thousand). Regarding the estimation performance over consecutive positions (third row), the bidirectional LSTM shows more competitive results. In this case, the bidirectional model with $M = 16$ is

TABLE III
UNI/BIDIRECTIONAL LSTM (TRAINED ON CONSECUTIVE)

	$M=32$		$M=16$	
	Unidir.	Bidir.	Unidir.	Bidir.
Num. parameters	17172	34324	7572	15124
$\overline{\text{MSE}}$ [dB^2] (ev. random)	1848	1811	2748	1969
$\overline{\text{MSE}}$ [dB^2] (ev. consec.)	56.36	44.69	54.07	44.99

selected as the best option, since doubling the parameters only improves the second decimal of the $\overline{\text{MSE}}$.

The complexity order of the proposed (unidirectional) LSTM scheme has two dominating terms: the complexity of the encoder (one LSTM cell with M units [28]) and the complexity of the decoder (a fully connected layer). The overall complexity order is given by $O(NM^2 + MN^2)$, where the dominant term depends on the relative magnitude between N and M. The computational complexity order of Ordinary Kriging is $\mathcal{O}(N^3)$ [29], due to the inversion of a semivariance matrix to compute the weights. If new points get measured and weights need to be updated, online solutions based on inverse matrix theory allow to get the new weights with a computational complexity of $\mathcal{O}(N^2)$. Once the weights are available, the evaluation of the REM in a new location with unknown REM value has a complexity order $\mathcal{O}(N)$, leading to a complexity order $\mathcal{O}(N^2)$ to reconstruct a complete sequence. Since the selected value of M in the LSTM is quite low ($M = 16$), as the number of samples to reconstruct grows, the complexity order is dominated by $\mathcal{O}(MN^2)$. Thus, our proposal leads to a DL-based REM reconstruction scheme suited for vehicular scenarios and of similar complexity to other methods such as Kriging.

IV. LOWER BOUND ANALYSIS

According to the model in Section II, the large-scale channel dynamics over a set of N positions can be modeled as a multivariate Gaussian distribution with probability density function (PDF):

$$f_{\mathbf{y}}(y_1,\ldots,y_N) = \frac{1}{\sqrt{(2\pi)^N|\boldsymbol{\Sigma}|}} \exp\left(\frac{-(\mathbf{y}-\boldsymbol{\mu})^{\mathrm{T}}\boldsymbol{\Sigma}^{-1}(\mathbf{y}-\boldsymbol{\mu})}{2}\right), \tag{8}$$

where $\mathbf{y} \sim \mathcal{N}(\boldsymbol{\mu}, \boldsymbol{\Sigma})$ is a random vector modeling the average received power readings at the considered locations, $\boldsymbol{\mu} \in \mathbb{R}^{N\times 1}$ is the vector collecting the corresponding mean values (i.e., averaging over space in the considered environment) and $\boldsymbol{\Sigma} \in \mathbb{R}^{N\times N}$ the covariance matrix, so that $y_i \in \mathcal{N}(\mu_i, \sigma_{ii}^2)$ and $\text{Cov}(y_i, y_j) = C_{ij}$. Operator $|\cdot|$ indicates the determinant. The power space profile described by the average values in μ can be easily derived from the path-loss model (4) and the BS distances to the N positions in $\mathbf{x}$. Similarly, the elements of $\boldsymbol{\Sigma}$ directly match the correlation values in (2).

Considering that in the problem to solve there are observations available for P out of the N random variables, the best estimate for the unknown components in the Bayesian sense, are those minimizing the Bayesian MSE, according to the minimum MSE (MMSE) criterion.

The posterior PDF takes the form of another multivariate Gaussian random variable with fewer components [30], with mean $\bar{\boldsymbol{\mu}} \in \mathbb{R}^{N-P}$ and covariance $\bar{\boldsymbol{\Sigma}} \in \mathbb{R}^{(N-P)\times(N-P)}$. The MMSE estimate is known to be the mean of such pdf [30].

The random vector $\mathbf{y} \in \mathbb{R}^{N\times 1}$ can be partitioned into two mutually exclusive subsets containing variables modeling field values at road locations with unavailable readings, $\mathbf{y}_{\mathcal{U}} \in \mathbb{R}^{(N-P)\times 1}$, and those corresponding to road locations with known values, $\mathbf{y}_{\mathcal{K}} \in \mathbb{R}^{P\times 1}$, where $\mathbf{y}_{\mathcal{U}}$ is dependent on $\mathbf{y}_{\mathcal{K}}$:

$$\mathbf{y} = [\mathbf{y}_{\mathcal{U}}\, \mathbf{y}_{\mathcal{K}}]^{\mathrm{T}}, \quad \boldsymbol{\mu} = [\boldsymbol{\mu}_{\mathcal{U}}\, \boldsymbol{\mu}_{\mathcal{K}}]^{\mathrm{T}}, \tag{9}$$

$$\boldsymbol{\Sigma} = \begin{bmatrix} \boldsymbol{\Sigma}_{\mathcal{U}\mathcal{U}} & \boldsymbol{\Sigma}_{\mathcal{U}.\mathcal{K}.} \\ \boldsymbol{\Sigma}_{\mathcal{K}\mathcal{U}} & \boldsymbol{\Sigma}_{\mathcal{K}\mathcal{K}} \end{bmatrix}. \tag{10}$$

Based on the partitions above, the posterior distribution of the unknown components given the known observations $\mathbf{z}$, $p(\mathbf{y}_{\mathcal{U}}|\mathbf{y}_{\mathcal{K}} = \mathbf{z})$, is a multivariate normal distribution with a mean vector $\bar{\boldsymbol{\mu}}$ and a new covariance matrix $\bar{\boldsymbol{\Sigma}}$ obtained as [30]:

$$\bar{\boldsymbol{\mu}} = \boldsymbol{\mu}_{\mathcal{U}} + \boldsymbol{\Sigma}_{\mathcal{U}.\mathcal{K}.}\boldsymbol{\Sigma}_{\mathcal{K}\mathcal{U}}^{-1}(\mathbf{z} - \boldsymbol{\mu}_{\mathcal{K}}) \tag{11}$$

$$\bar{\boldsymbol{\Sigma}} = \boldsymbol{\Sigma}_{\mathcal{U}\mathcal{U}} - \boldsymbol{\Sigma}_{\mathcal{U}.\mathcal{K}.}\boldsymbol{\Sigma}_{\mathcal{K}\mathcal{K}}^{-1}\boldsymbol{\Sigma}_{\mathcal{K}\mathcal{U}}. \tag{12}$$

As a result, the values in $\bar{\boldsymbol{\mu}}$ provide the MMSE estimate minimizing the global average MSE in (7). The resulting MSE provides, for each case, a meaningful performance lower bound of the problem at hand equal to

$$\text{MSE}_{\text{LB}} = \frac{1}{N-P}\text{Tr}(\bar{\boldsymbol{\Sigma}}), \tag{13}$$

where $\text{Tr}(\cdot)$ denotes the trace of a matrix.

Note that, in general, there are C_P possible ways of splitting $\mathbf{y}$ and each combination leads to a different MSE_{LB}. Therefore, for a given N and P we evaluate the average MSE as:

$$\overline{\text{MSE}}_{\text{LB}} = \frac{1}{C_P}\sum_{c}\text{MSE}_{\text{LB}}^{(c)}, \tag{14}$$

where $\text{MSE}_{\text{LB}}^{(c)}$ denotes the lower bound of the error for a particular combination c.

V. NUMERICAL RESULTS

A. 3GPP Freeway Scenario

First, the proposed channel reconstruction method has been evaluated on a synthetically generated dataset of similar characteristics to those already used for training and testing the network, but containing different elements. To evaluate the trade-off between the reduction of signaling when estimating the N channel values versus the quality of the estimation (evaluated using the MSE), a sweep of the number of known samples has been made between $P = 3$ and $P = 19$. Data have also been generated for different values of decorrelation distances $L_c \in [25, 50]$. For all the combinations of parameters, the theoretical lower bound on the MSE is also calculated. Finally, the performance of the Ordinary Kriging interpolation algorithm has been included in the evaluation, in order to have the benchmark of a widely known non-DL-based REM reconstruction algorithm. Fig. 3 shows the resulting MSE after averaging 1000

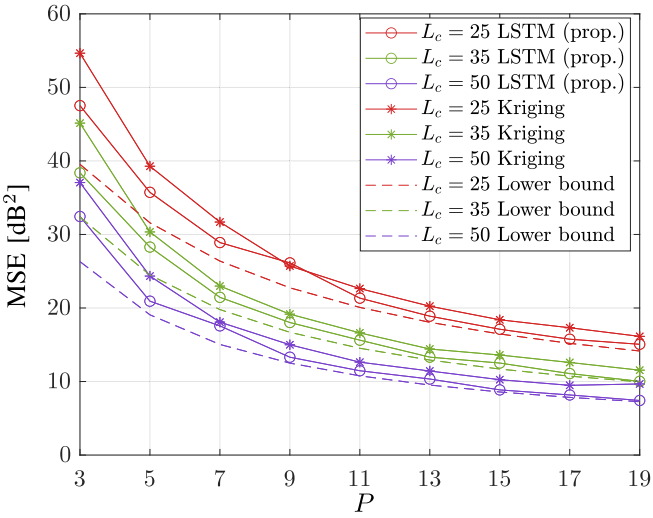

Fig. 3. Average MSE comparison considering all the possible combinations of missing values for each P.

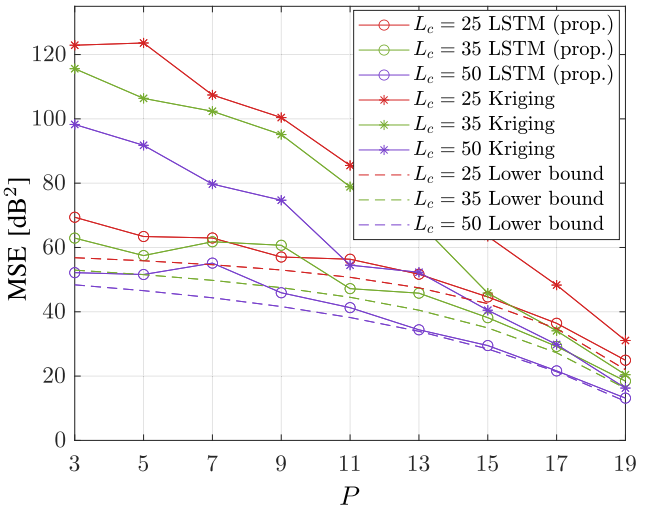

Fig. 4. Average MSE comparison considering only the combinations where the first P values are known (consecutive combinations).

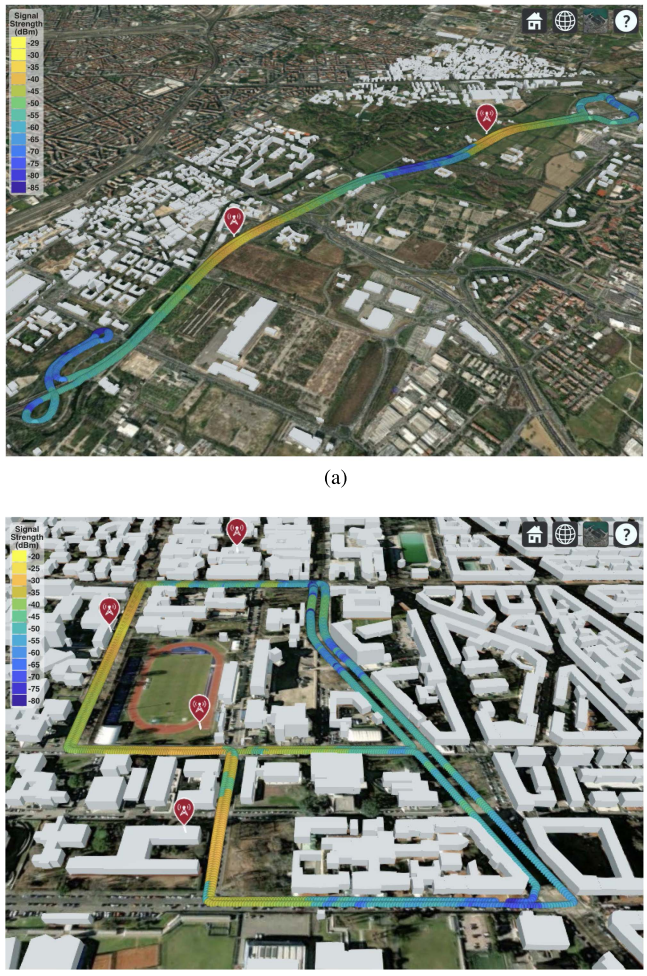

(a)

(b)

Fig. 5. Simulated trajectory in (a) freeway and (b) urban scenarios in Milan, Italy. The trajectory is colored according to the value of received power. Red markers indicate 5G BS locations. (a) Freeway. (b) Urban.

realizations of the shadowing random vector for each of the C_P possible random combinations of known values. We can clearly see that the proposed unidirectional LSTM with $M = 16$ outperforms the Kriging algorithm in terms of MSE, getting very close to, and sometimes reaching, the theoretical lower bound of the problem. For instance, the performance of the network for $L_c = 50$ m overlaps with the lower bound for $P \geq 15$.

Fig. 4 shows the MSE results versus the value of P, considering only the combination with the first P consecutive known values for each case. Each MSE value is the result of averaging 1000 realizations of the shadowing random vector. The results with the proposed bidirectional LSTM model with $M = 16$ trained with consecutive samples are shown to be very close to the theoretical lower bound of the problem, mainly for $P \geq 13$. The Ordinary Kriging method presents a substantial performance loss when a set of consecutive known samples are considered instead of samples in random positions. The latter result is consistent with the conclusion extracted in [5] about the combinations of samples minimizing the MSE, where the optimal combinations contained the first and last samples in most cases.

B. Milan Urban and Freeway Scenarios

In order to assess the generalization capabilities of the proposed neural network over unseen or unknown settings, the model was tested over propagation data coming from simulations in two distinct realistic scenarios in Milan (Italy), as shown in Fig. 5. In the urban scenario, four 5G BSs are deployed, while in the freeway two BSs are located along a 2 km section road. Vehicles move at a constant speed of 50 km/h and 80 km/h in the two scenarios, respectively.

Wireless InSite 3D prediction software [31] is used to simulate signal propagation from the BSs to the vehicles, enabling realistic 3D ray-tracing simulations thanks to its integration with the OpenStreetMap database. The software models the physical

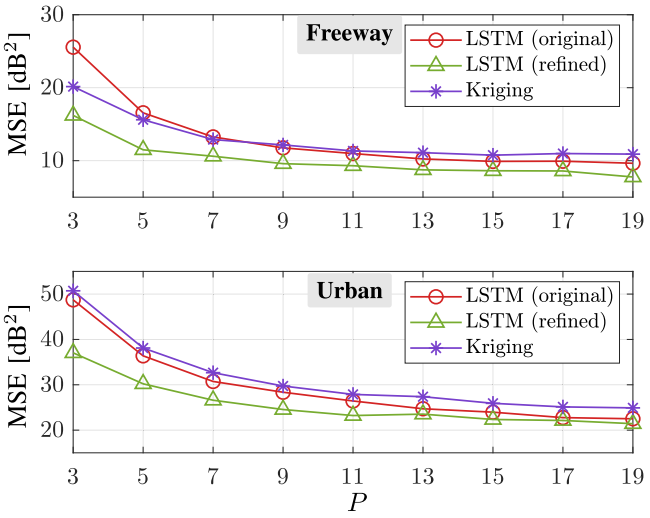

Fig. 6. MSE comparison considering data from two realistic freeway and urban scenarios in Milan.

characteristics of irregular terrain and urban building features (such as permittivity, conductivity, roughness, and thickness) by accounting for electromagnetic properties through the Uniform Theory of Diffraction (UTD). It supports ray-based solvers and handles up to fifty paths.

Both the UE and BSs transmission-reception points (TRPs) are equipped with one isotropic antenna. This is done in order to avoid any alteration of the received power due to array gains. Regarding the values of $V(\mathbf{x}_i)$, for each vehicle position we consider the highest received power out of all the BSs. Note that, the received power generated by the 3D simulation tool is also affected by small-scale effects such as the Doppler effect. In this case, the Doppler effect is motivated by the vehicle's movement with respect to the transmitter. Recall that in this work small-scale effects are assumed to be averaged out by the receiver. Channel loss samples have been taken along the paths shown in Fig. 5, considering a sample every 0.5 m. From the set of available values, the data set is composed of random realizations of groups of samples spaced 5 m apart and covering 100 m spans, as required by the problem.

The performance results obtained on the data generated in the two realistic Milan scenarios described above are presented in Fig. 6, where the average MSE values considering all the possible combinations of missing values for each P are represented. It can be observed that the LSTM model is able to perform the power field reconstruction even with data not following the 3GPP model considered for training. In the freeway scenario, the Kriging algorithm prediction performs better for $P < 7$, while the proposed LSTM is more competitive for higher P values. When considering the realistic urban scenario data (bottom panel of Fig. 6), the neural network is in all cases more competitive than the Kriging algorithm. The MSE values obtained in the freeway scenario are substantially lower than those in the urban scenario. The main difference between the freeway and urban environments data is that the latter present higher variability, with more often power drops which increase the shadowing variance and reduce the shadowing correlation distance. When comparing the results in Fig. 6 with the lower bounds represented in Fig. 3, it can be further observed that, for the freeway scenario, the MSE values resemble the theoretical lower bound calculated for the 3GPP scenario with $L_c = 50$ m, whereas, for the urban case, the values approach more the ones of the 3GPP scenario with $L_c = 25$ m. These results are consistent, since the shadowing correlation distance in urban scenarios is generally lower than in freeways.

In order to exploit the potential of ML-based approaches, we also present refined results for the two panels shown in Fig. 6, which we denote as 'LSTM (refined)'. These new results correspond to a fine-tuned version of the proposed LSTM model that has been adapted to a small fraction of the data (20%) observed in the two discussed scenarios. By departing from the model trained on 3GPP-compliant synthetic data, we are able to employ a transfer learning approach to update its weights using a small set of real data. The refined LSTM version produces a significant performance improvement, as shown in the updated Fig. 6.

VI. Conclusion

This work considered the problem of estimating a set of unknown large-scale channel values for the communication between a base station and vehicles travelling along a freeway. A low-complexity deep-learning-based estimation method is proposed, which considers a Long-Short Term Memory (LSTM) architecture with a reduced number of parameters, to guarantee a low-complexity radio map reconstruction.

The neural network has been trained with samples generated from a simplified path-loss model with random shadowing, using the parameters of 3GPP-compliant freeway scenario. For all the variations of parameters, the mean squared error (MSE) of the reconstructed values has been compared to its theoretical lower bound and to the classical Kriging algorithm for spatial interpolation. It can be observed that the LSTM model outperforms the Kriging method, and it is very close to the theoretical lower bound, reaching it in some cases.

Furthermore, the proposed model is able to generalize and perform the estimation with channel data generated in more realistic environments, specifically, considering the geometry and buildings of both urban and freeway settings in the city of Milan. Further work includes extensions of our proposal capable of performing two-dimensional REM reconstruction.

References

[1] V. Chowdappa, C. Botella, J.-J. Samper-Zapater, and R.-J. Martinez, "Distributed radio map reconstruction for 5G automotive," *IEEE Intell. Transp. Syst. Mag.*, vol. 10, no. 2, pp. 36–49, Summer 2018.

[2] H.-B. Yilmaz, T. Tugcu, F. Alagöz, and S. Bayhan, "Radio environment map as enabler for practical cognitive radio networks," *IEEE Commun. Mag.*, vol. 51, no. 12, pp. 162–169, Dec. 2013.

[3] P. Kryszkiewicz, A. Kliks, L. Kułacz, H. Bogucka, G.-P. Koudouridis, and M. Dryjański, "Context-based spectrum sharing in 5G wireless networks based on radio environment maps," *Wireless Commun. Mobile Comput.*, vol. 2018, pp. 1–15, Nov. 2018.

[4] M. Noor-A-Rahimet al., "6G for Vehicle-to-Everything (V2X) communications: Enabling technologies, challenges, and opportunities," *Proc. IEEE*, vol. 110, no. 6, pp. 712–734, Jun. 2022.

[5] S. Roger, C. Botella, J. J. Pérez-Solano, and J. Perez, "Application of radio environment map reconstruction techniques to platoon-based cellular V2X communications," *Sensors*, vol. 20, no. 9, 2020, Art. no. 2440. [Online]. Available: https://www.mdpi.com/1424-8220/20/9/2440
[6] R.-C. Dwarakanath, J.-D. Naranjo, and A. Ravanshid, "Modeling of interference maps for licensed shared access in LTE-advanced networks supporting carrier aggregation," in *Proc. IFIP Wireless Days*, 2013, pp. 1–5.
[7] H. Yilmaz and T. Tugcu, "Location estimation-based radio environment map construction in fading channels," *Wireless Commun. Mobile Comput.*, vol. 15, no. 3, pp. 561–570, Feb. 2015.
[8] S. Üreten, A. Yongaçoğlu, and E. Petriu, "A comparison of interference cartography generation techniques in cognitive radio networks," in *Proc. IEEE Int. Conf. Commun.*, 2012, pp. 1879–1883.
[9] R.-D. Taranto, S. Muppirisetty, R. Raulefs, D. Slock, T. Svensson, and H. Wymeersch, "Location-aware communications for 5G networks: How location information can improve scalability, latency, and robustness of 5G," *IEEE Signal Process. Mag.*, vol. 31, no. 6, pp. 102–112, Nov. 2014.
[10] V.-P. Chowdappa, M. Fröhle, H. Wymeersch, and C. Botella, "Distributed channel prediction for multi-agent systems," in *Proc. IEEE Int. Conf. Commun.*, 2017, pp. 1–6.
[11] N. D. Fabbro, M. Rossi, G. Pillonetto, L. Schenato, and G. Piro, "Model-free radio map estimation in massive MIMO systems via semi-parametric Gaussian regression," *IEEE Wireless Commun. Lett.*, vol. 11, no. 3, pp. 473–477, Mar. 2022.
[12] E. Dall'Anese, S.-J. Kim, and G. Giannakis, "Channel gain map tracking via distributed Kriging," *IEEE Trans. Veh. Technol.*, vol. 60, no. 3, pp. 1205–1211, Mar. 2011.
[13] H. Braham, S.-B. Jemaa, G. Fort, E. Moulines, and B. Sayrac, "Spatial prediction under location uncertainty in cellular networks," *IEEE Trans. Wireless Commun.*, vol. 15, no. 11, pp. 7633–7643, Nov. 2016.
[14] K. Sato and T. Fujii, "Kriging-based interference power constraint: Integrated design of the radio environment map and transmission power," *IEEE Trans. Cogn. Commun. Netw.*, vol. 3, no. 1, pp. 13–25, Mar. 2017.
[15] Z. Han, J. Liao, Q. Qi, H. Sun, and J. Wang, "Radio environment map construction by Kriging algorithm based on mobile crowd sensing," *Wireless Commun. Mobile Comput.*, vol. 2019, pp. 1–12, Feb. 2019.
[16] K. Sato, K. Inage, and T. Fujii, "On the performance of neural network residual Kriging in radio environment mapping," *IEEE Access*, vol. 7, pp. 94557–94568, 2019.
[17] K. Suto, S. Bannai, K. Sato, K. Inage, K. Adachi, and T. Fujii, "Image-driven spatial interpolation with deep learning for radio map construction," *IEEE Wireless Commun. Lett.*, vol. 10, no. 6, pp. 1222–1226, Jun. 2021.
[18] S. Shrestha, X. Fu, and M. Hong, "Deep spectrum cartography: Completing radio map tensors using learned neural models," *IEEE Trans. Signal Process.*, vol. 70, pp. 1170–1184, 2022.
[19] D. Romero and S.-J. Kim, "Radio map estimation: A data-driven approach to spectrum cartography," *IEEE Signal Process. Mag.*, vol. 39, no. 6, pp. 53–72, Nov. 2022.
[20] Y. Reddy, A. Kumar, O. Pandey, and L. Cenkeramaddi, "Spectrum cartography techniques, challenges, opportunities, and applications: A survey," *Pervasive Mobile Comput.*, vol. 79, Jan. 2022, Art. no. 101511. [Online]. Available: https://www.sciencedirect.com/science/article/pii/S1574119221001346
[21] R. Levie, C. Yapar, G. Kutyniok, and G. Caire, "RadioUNet: Fast radio map estimation with convolutional neural networks," *IEEE Trans. Wireless Commun.*, vol. 20, no. 6, pp. 4001–4015, Jun. 2021.
[22] W. Yin, K. Kann, M. Yu, and H. Schütze, "Comparative study of CNN and RNN for natural language processing," 2017, *arXiv:1702.01923*.
[23] 3rd Generation Partnership Project TSG RAN, "Study on LTE-based V2X services," 3GPP, Sophia Antipolis, France, Tech. Rep. 36.885 V14.0.0, 2016.
[24] A. Goldsmith, *Wireless Communications*. Cambridge, MA, USA: Cambridge Univ. Press, 2005.
[25] M. Gudmunson, "Correlation model for shadow fading in mobile radio systems," *Electron. Lett.*, vol. 27, no. 23, pp. 2145–2146, Nov. 1991.
[26] K. Katagiri, K. Sato, and T. Fujii, "Crowdsourcing-assisted radio environment database for V2V communication," *Sensors*, vol. 2018, no. 18, pp. 1–17, Apr. 2018.
[27] D. P. Kingma and J. Ba, "Adam: A method for Stochastic optimization," in *Proc. Int. Conf. Learn. Representations*, San Diego, USA, 2015.
[28] P. J. Freire, S. Srivallapanondh, A. Napoli, J. E. Prilepsky, and S. K. Turitsyn, "Computational complexity evaluation of neural network applications in signal processing," 2022, *arXiv:2206.12191*.
[29] N.-A.-C. Cressie, *Statistics for Spatial Data*. Hoboken, NJ, USA: Wiley, 1993.
[30] Y. L. Tong, *The Multivariate Normal Distribution*. Berlin, Germany: Springer, 2012.
[31] Remcom Inc., "Wireless InSite 3D wireless prediction software," 2023. [Online]. Available: https://www.remcom.com/wireless-insite-em-propagation-software

Sandra Roger (Senior Member, IEEE) received the Ph.D. degree in telecommunications engineering from the Universitat Politècnica de València (UPV), Valencia, Spain, in 2012. During doctorate studies, she performed two research stays with the Institute of Telecommunications, Vienna University of Technology, Vienna, Austria. From 2012 to 2018, she was a Senior Researcher with the iTEAM Research Institute, UPV, where she worked in the European projects METIS and METIS-II on 5G design. In 2019, she joined the Computer Science Department of the Universitat de València, where she is currently an Associate Professor. Dr. Roger has authored/coauthored more than 60 papers in renowned conferences and journals. Her research interests include the field of signal processing for communications, vehicular communications, and wireless system design.

Mattia Brambilla (Member, IEEE) received the B.Sc. and M.Sc. degrees in telecommunication engineering and the Ph.D. degree (*cum laude*) in information technology from the Politecnico di Milano, Milan, Italy, in 2015, 2017, and 2021, respectively. He was a Visiting Researcher with the NATO Centre for Maritime Research and Experimentation, La Spezia, Italy, in 2019. In 2021, he joined the faculty of Dipartimento di Elettronica, Informazione e Bioingegneria (DEIB), Politecnico di Milano as Research Fellow. His research interests include signal processing, statistical learning, and data fusion for cooperative localization and communication. He was the recipient of the Best Student Paper Award at the 2018 IEEE Statistical Signal Processing Workshop.

Bernardo Camajori Tedeschini (Graduate Student Member, IEEE) received the B.Sc. (Hons.) in computer science and M.Sc. (Hons.) degrees in telecommunications engineering from the Politecnico di Milano, Milan, Italy, in 2019 and 2021, respectively. Since November 2021, he has been a Ph.D. Fellow in information technology with Dipartimento di Elettronica, Informazione e Bioingegneria, Politecnico di Milano. He is currently a Visiting Researcher with the Laboratory for Information & Decision Systems, the Massachusetts Institute of Technology, Cambridge, MA, USA. His research interests include federated learning, machine learning, and localization methods. He was the recipient of the Ph.D. grant from the ministry of the Italian government Ministero dell'Istruzione, Rome, Italy, dell'Universitá e della Ricerca (MIUR), Pescara, Italy, and the Roberto Rocca Doctoral Fellowship granted by MIT and Politecnico di Milano, Milan, Italy.

Carmen Botella-Mascarell (Senior Member, IEEE) received the M.Sc. and Ph.D. degrees in telecommunications engineering from Universitat Politècnica de València, Valencia, Spain, in 2003 and 2008, respectively. In 2009 and 2010, she was a Postdoctoral Researcher with the Communications Systems and Information Theory group, Chalmers University of Technology, Gothenburg, Sweden. In 2011, she joined the Computer Science Department, Universitat de València, Valencia, where she is currently an Associate Professor. Dr Botella-Mascarell has authored/coauthored 75 technical papers in international conferences and journals. Her research interests include the general areas of coordination and cooperation in wireless systems, with special focus on physical-layer solutions for 5G and beyond.

Maximo Cobos (Senior Member, IEEE) received the master's degree in telecommunications and the Ph.D. degree in telecommunications engineering from the Universitat Politècnica de València, Valencia, Spain, in 2007 and 2009, respectively. He completed with honors his studies from the University Faculty Training Program. In 2011, he joined the Universitat de València, Valencia, where he is currently a Full Professor. From 2009 to 2011, he was a Guest Researcher with T-Labs Berlin, Berlin, Germany and in 2019 with Politecnico di Milano, Milan, Italy, where he also held an Adjunct Professorship from 2020 to 2021. His research interests include the area of digital signal processing and machine learning for wireless sensor networks, audio and multimedia applications, where he has authored or coauthored more than 100 technical papers in international journals and conferences. He was the recipient of the Ericsson Best Ph.D. Thesis Award from Spanish National Telecommunications Engineering Association. In 2010, was also the recipient of Campus de Excelencia Postdoctoral Fellowship to work with the iTEAM Research Institute, Valencia. He is a Member of the Audio Signal Processing Technical Committee of the European Acoustics Association and an Associate Editor for the IEEE SIGNAL PROCESSING LETTERS.

Monica Nicoli (Senior Member, IEEE) received the M.Sc. (Hons.) and Ph.D. degrees in communication engineering from Politecnico di Milano, Milan, Italy, in 1998 and 2002, respectively. She was a Visiting Researcher with ENI Agip, Rome, Italy, from 1998 to 1999 and Uppsala University, Uppsala, Sweden, in 2001. In 2002, she was with Politecnico di Milano as a Faculty Member. She is currently an Associate Professor in telecommunications with the Department of Management, Economics and Industrial Engineering. Her research interests include signal processing, machine learning, and wireless communications, with emphasis on smart mobility and Internet of Things (IoT). She was the recipient of the Marisa Bellisario Award, in 1999 and Co-recipient of the best paper awards of the EuMA Mediterranean Microwave Symposium, in 2022, the IEEE Symposium on Joint Communications and Sensing, in 2021, the IEEE Statistical Signal Processing Workshop, in 2018, and the IET Intelligent Transport Systems journal, in 2014. She is an Associate Editor of the IEEE Transactions on Intelligent Transportation Systems. She was also an Associate Editor for the *EURASIP Journal on Wireless Communications and Networking*, from 2010 to 2017 and a Lead Guest Editor for the Special Issue on Localization in Mobile Wireless and Sensor Networks, in 2011.